

Compression Behavior of Single-layer Graphenes

Otakar Frank¹, Georgia Tsoukleri^{1,2}, John Parthenios^{1,2}, Konstantinos Papagelis³, Ibtsam

Riaz⁴, Rashid Jalil⁴, Kostya S. Novoselov⁴, and Costas Galiotis^{1,2,3}

Supporting Information

Raman study of graphene - background

The recently developed method for graphene preparation by micromechanical cleavage of graphite¹ provides an opportunity for studying the Raman band shifts of both G and 2D modes^{2,3} upon tensile or compressive loading at the molecular level.⁴⁻⁹ This is important not only for highlighting the extreme strength and stiffness of graphene but also to link its behaviour with the mechanical deformation of other graphitic structures such as bulk graphite, carbon nanotubes (CNT) and CF. The G peak corresponds to the doubly degenerate E_{2g} phonon at the Brillouin zone centre. The D peak is due to the breathing modes of sp^2 rings and requires a defect for its activation.^{2,3,10} It comes from TO phonons around the **K** point of the Brillouin zone, is active by double resonance¹¹ and is strongly dispersive with excitation energy due to a Kohn Anomaly at **K**.¹² The 2D peak is the second order of the D peak. This is a single peak in monolayer graphene, whereas it splits in four in bilayer graphene, reflecting the evolution of the band structure.^{2,3} Since the 2D peak originates from a process where momentum conservation is obtained by the participation of two phonons with opposite wavevectors it does not require the presence of defects for its activation, and is thus always present. Indeed, high quality graphene shows the G, 2D peaks, but not D.

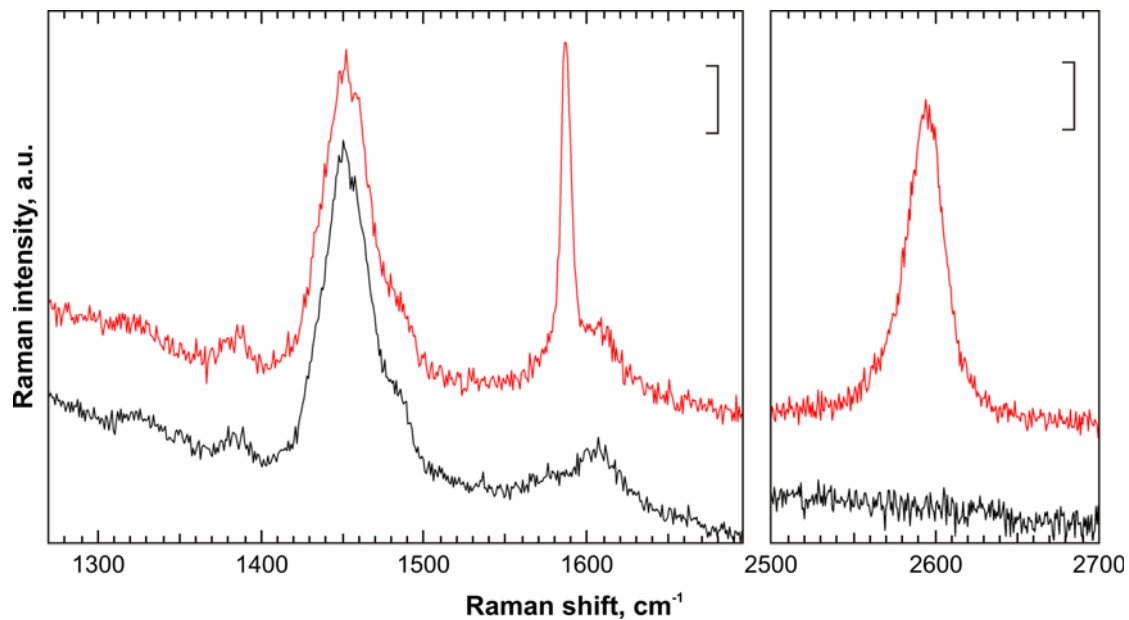


Figure S1. Original Raman spectra excited by a 785 nm laser of the combined SU8 and S1805 substrate (black) and a graphene flake embedded within this substrate (red). The spectra are offset for clarity, and scale bars represent 500 counts in both panels.

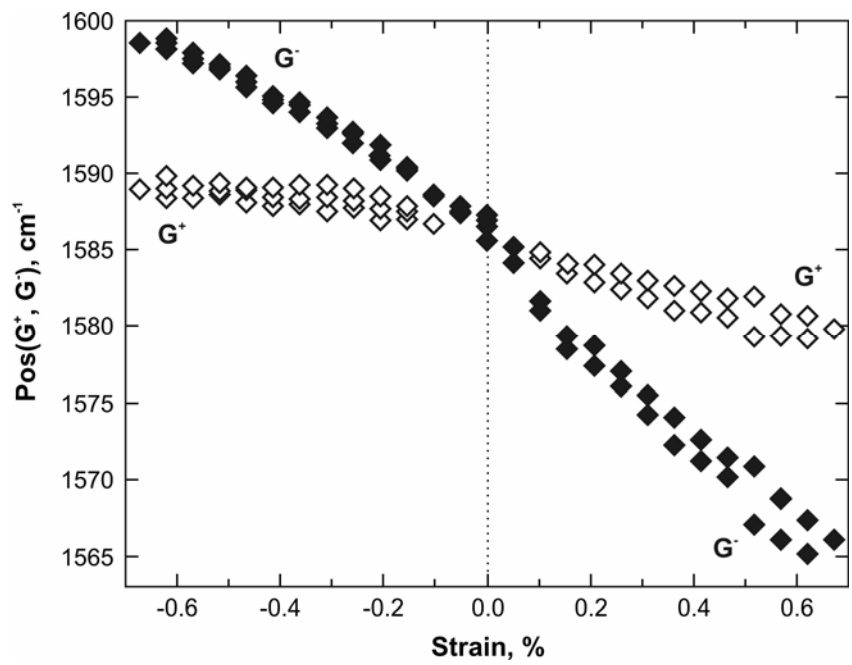


Figure S2. Plot of G band positions as a function of strain from experiments conducted of flake F1 (Figure 1c, main text). Strain with positive (negative) values indicates tension (compression). Full end empty diamonds indicate the frequency position of the G^- and G^+ subbands.

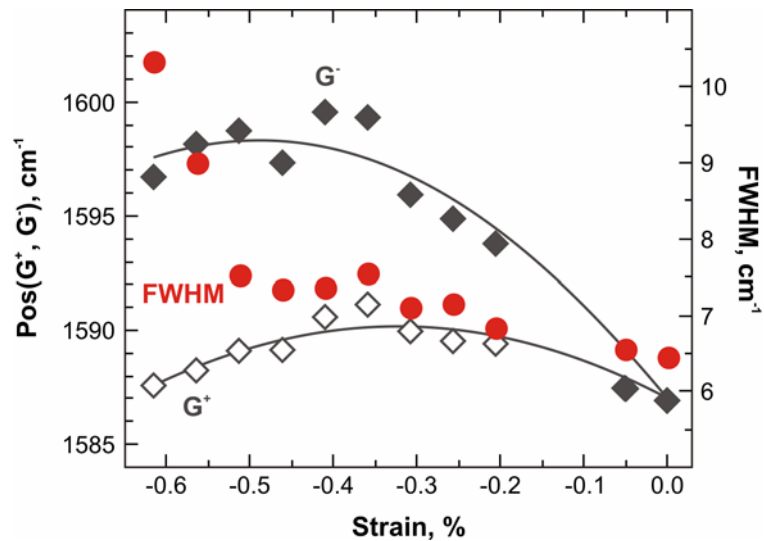


Figure S3. Plot of G^- and G^+ band positions and their FWHM as a function of strain on a selected spot on flake F2 (Fig. 1c, main text). Full circles indicate the bands' FWHM (right axis), full (empty) diamonds show the position of the G^- (G^+) sub-bands. Only one set of FWHM is presented, since both sub-bands have the same width for a given strain level. Solid (dashed) lines are 2nd order polynomial fits of the $G^-(G^+)$ band position measurements.

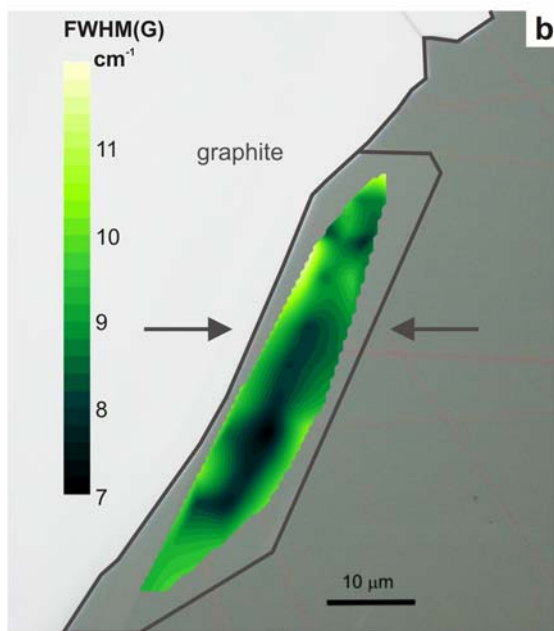
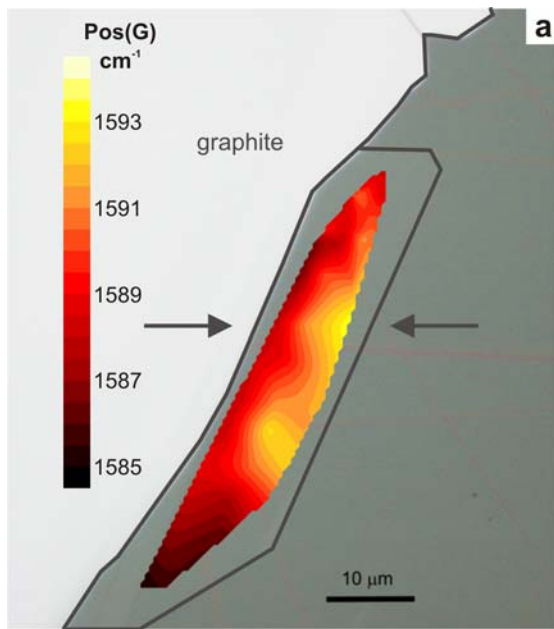


Figure S4. Post mortem (a) $\text{Pos}(\text{G})$ and (b) $\text{FWHM}(\text{G})$ maps of specimen F2 after cyclic loading. The band was fitted as a single Lorentzian. The light grey area in both (a) and (b) corresponds to bulk graphite. The arrows indicate the strain direction.

		G⁻		G⁺	
	a ₀	a ₁	a ₂	a ₁	a ₂
F1					
1	1586.9	-22.5 ± 0.9	-5.9 ± 1.8	-1.8 ± 1.0	1.4 ± 1.9
2	1587.3	-18.8 ± 0.8	-2.5 ± 1.6	-4.0 ± 0.9	-1.94 ± 1.7
3	1586.5	-25.2 ± 1.0	-9.9 ± 2.0	-10.5 ± 1.2	-9.54 ± 2.4
F2					
1	1585.1	-36.1 ± 1.8	-28.9 ± 3.8	-12.2 ± 0.8	-17.14 ± 1.6
2	1584.6	-34.1 ± 2.8	-24.1 ± 6.1	-13.0 ± 1.4	-18.2 ± 3.1
3	1583.3	-28.4 ± 1.0	-13.0 ± 2.2	-4.5 ± 1.0	-0.7 ± 2.2
2D					
	a ₀	a ₁	a ₂		
F1					
1	2956.5	-38.0 ± 2.1	-10.3 ± 4.1		
2	2596.6	-36.6 ± 3.4	-13.5 ± 6.3		
3	2594.6	-41.7 ± 3.2	-12.6 ± 6.4		
F2					
1	2592.3	-59.8 ± 4.5	-52.4 ± 9.8		
2	2591.3	-60.1 ± 7.6	-54.8 ± 16.6		
3	2598.4	-45.4 ± 7.8	-19.9 ± 17.2		

Table S1. Coefficients of 2nd order polynomial curves fitted to the Raman G⁺, G⁻ and 2D bands evolution with compressive strain. The fit equation can be written: $\omega = a_0 + a_1 |\varepsilon| - a_2 \varepsilon^2$. Thus $a_0 = \omega^0$ (cm⁻¹), a₁ corresponds to the strain sensitivity $\partial_{G,2D}/\partial\varepsilon$ (cm⁻¹/%) close to zero strain, and a₂ expresses the curvature of the slope $\partial_{G,2D}/\partial\varepsilon^2$ (cm⁻¹/%)²). The ± sign prefaces a value of 95% confidence interval.

Supporting Information References

1. Novoselov, K. S.; Geim, A. K.; Morozov, S. V.; Jiang, D.; Zhang, Y.; Dubonos, S. V.; Grigorieva, I. V.; Firsov, A. A. *Science* **2004**, *306* (5296), 666-669.
2. Ferrari, A. C.; Meyer, J. C.; Scardaci, V.; Casiraghi, C.; Lazzeri, M.; Mauri, F.; Piscanec, S.; Jiang, D.; Novoselov, K. S.; Roth, S.; Geim, A. K. *Phys. Rev. Lett.* **2006**, *97* (18), 187401.
3. Malard, L. M.; Pimenta, M. A.; Dresselhaus, G.; Dresselhaus, M. S. *Phys. Rep.* **2009**, *473* (5-6), 51-87.
4. Huang, M. Y.; Yan, H. G.; Chen, C. Y.; Song, D. H.; Heinz, T. F.; Hone, J. *Proc. Natl. Acad. Sci. U.S.A.* **2009**, *106* (18), 7304-7308.
5. Mohiuddin, T. M. G.; Lombardo, A.; Nair, R. R.; Bonetti, A.; Savini, G.; Jalil, R.; Bonini, N.; Basko, D. M.; Galiotis, C.; Marzari, N.; Novoselov, K. S.; Geim, A. K.; Ferrari, A. C. *Phys. Rev. B* **2009**, *79* (20), 205433-8.
6. Ni, Z. H.; Yu, T.; Lu, Y. H.; Wang, Y. Y.; Feng, Y. P.; Shen, Z. X. *Acs Nano* **2008**, *2* (11), 2301-2305.
7. Proctor, J. E.; Gregoryanz, E.; Novoselov, K. S.; Lotya, M.; Coleman, J. N.; Halsall, M. P. *Phys. Rev. B* **2009**, *80* (7), 073408-4.
8. Yu, T.; Ni, Z. H.; Du, C. L.; You, Y. M.; Wang, Y. Y.; Shen, Z. X. *J. Phys. Chem. C* **2008**, *112* (33), 12602-12605.
9. Tsoukleri, G.; Parthenios, J.; Papagelis, K.; Jalil, R.; Ferrari, A. C.; Geim, A. K.; Novoselov, K. S.; Galiotis, C. *Small* **2009**, *5* (21), 2397-2402.
10. Tuinstra, F.; Koenig, J. L. *The Journal of Chemical Physics* **1970**, *53* (3), 1126-1130.
11. Maultzsch, J.; Reich, S.; Thomsen, C. *Phys. Rev. B* **2004**, *70* (15), 155403.
12. Piscanec, S.; Lazzeri, M.; Mauri, F.; Ferrari, A. C.; Robertson, J. *Phys. Rev. Lett.* **2004**, *93* (18).